LIMNOLOGY and OCEANOGRAPHY

ASLO

Limnol. Oceanogr. 65, 2020, 224–235

doi: 10.1002/lno.11293

Effects of seasonal upwelling and runoff on water chemistry and growth and survival of native and commercial oysters

Jordan A. Hollarsmith [1,2*] Jason S. Sadowski,[1,2] Manon M. M. Picard,[1,3] Brian Cheng,[1,4] James Farlin,[1,5] Ann Russell,[1,6] Edwin D. Grosholz[1,2]

[1]Bodega Marine Laboratory, University of California, Bodega Bay, California
[2]Department of Environmental Science and Policy, University of California, Davis, California
[3]Department of Biology, Laval University, Quebec, Quebec, Canada
[4]Department of Environmental Conservation, University of Massachusetts, Amherst, Massachusetts
[5]Elementar Americas, Mt Laurel, New Jersey
[6]Department of Earth and Planetary Sciences, University of California, Davis, California

Abstract

The effects of climate change, including ocean acidification and ocean heatwaves, on biological communities in estuaries are often uncertain. Part of the uncertainty is due to the complex suite of environmental factors in addition to acidification and warming that influence the growth of shells and skeletons of many estuarine organisms. The goal of this study was to document spatial and temporal variation in water column properties and to measure the in situ effects on larval and recently settled stages of ecologically important Olympia oysters (*Ostrea lurida*) and commercially important Pacific oysters (*Crassostrea gigas*) in a low-inflow estuary with a Mediterranean climate in Northern California. Our results reveal that seasonal inputs of upwelled or riverine water create important and predictable gradients of carbonate system parameters, temperature, salinity, dissolved oxygen (DO), and other variables that influence oyster performance, and that the influence of these gradients is contingent upon the location in the estuary as well as seasonal timing. During upwelling events (dry season), temperature, carbonate chemistry, and DO had the greatest impact on oyster performance. During runoff events (wet season), gradients in salinity, nutrient concentrations, and total alkalinity driven by river discharge were comparatively more important. These results suggest that the spatial importance of carbonate chemistry and temperature are seasonally variable and are two of several other factors that determine oyster performance. We use these results to discuss future impacts on oysters given projected regional changes in the frequency and magnitude of upwelling and precipitation-driven runoff events.

Acidification and warming of the world's oceans are at the forefront of concerns regarding the health of coastal ecosystems. Since the onset of industrialization, atmospheric CO_2 has increased by 30% (Feely et al. 2004, 2008). This has driven an increase of ~ 0.6°C in mean global sea surface temperature (Hirahara et al. 2014), and increases in marine pCO_2 have reduced pH values in the global oceans by ~ 0.1 unit (Sabine et al. 2004). However, the processes governing rates of acidification in estuaries are especially complex. Previous work has documented that carbonate chemistry in estuarine habitats can be strongly influenced by advection of corrosive upwelled waters from coastal oceans (Banas et al. 2007), inputs of low-alkalinity freshwater from streams and rivers in the surrounding watersheds (Smith et al. 1991; Smith and Hollibaugh 1997; Yao and Hu 2017), and diel cycling of plant photosynthesis and respiration (Wootton et al. 2008). Concurrent with these biological- and event-driven changes to carbonate chemistry are considerable spatial and temporal variation in other water column parameters, including temperature, dissolved oxygen (DO), salinity, and food availability. Much work has demonstrated the ecological importance of multiple stressors acting in concert, highlighting the potential vulnerability of estuarine organisms to climate change (Breitburg et al. 2015). Thus, measuring the impacts of acidification and increased temperature, relative to other water column variables, on estuarine species requires understanding spatial and temporal variation in water column properties along seasonally variable estuarine gradients.

Among the more important estuarine species at risk from changing water column properties are Olympia (*Ostrea lurida*) and Pacific (*Crassostrea gigas*) oysters. Olympia oysters are important foundation species endemic to western North American estuaries. Pacific oysters originate from the Asian Pacific coast but are found

*Correspondence: jahollarsmith@ucdavis.edu

Additional Supporting Information may be found in the online version of this article.

in temperate waters globally, either in commercial aquaculture or as invaders in natural systems (Herbert et al. 2016). Although there has been considerable work on the impacts of carbonate chemistry on commercial Pacific oysters (e.g., Barton et al. 2012), and limited work with Olympia oysters (Hettinger et al. 2012, 2013; Waldbusser et al. 2016), most of this research has taken place in laboratory and mesocosm settings where individual drivers are easily controlled and their impacts carefully measured. In natural settings, however, changes in carbonate chemistry do not happen in isolation, and oysters have been shown to be vulnerable to changes in temperature, salinity, DO, and food availability (Kimbro et al. 2009*b*; Wasson 2010; Hettinger et al. 2013; Cheng et al. 2015). Thus, field studies are necessary to link natural variation in the full range of water column variables with population responses of target species (Andersson et al. 2015; Breitburg et al. 2015).

Consequently, our goal was to determine the in situ effects of seasonal and spatial water column variability on the performance of two oyster species in a Northern California estuary. This field-based approach allowed us to directly link variation in biologically relevant water column parameters with variation in the growth and survival of individual oysters. We measured water column parameters at several depths and distances from the mouth of the estuary during the three seasonal periods of low-inflow estuaries: upwelling (spring/summer), relaxation (summer/fall), and runoff (winter) (García-Reyes and Largier 2012). Parameters measured included temperature, salinity, DO, carbonate system (pH, dissolved inorganic carbon [DIC], pCO_2, total alkalinity [T_{alk}]), dissolved inorganic nitrogen (DIN; NO_2, NH_4^+, NO_3^-), phosphate (PO_4^{3-}), and phytoplankton biomass (chlorophyll *a*). We then used statistical modeling to determine the degree to which spatial and temporal variation in water column characteristics predicts oyster growth and survival.

Methods

Site description

Tomales Bay (38.15°N, 122.90°W) is a 20 km-long linear estuary with a mean width of 1.4 km, located approximately 70 km north of San Francisco Bay, CA. The bay is characterized as a low-inflow drowned river estuary in a Mediterranean climate with oceanography and biogeochemistry that vary strongly by season and location along the estuarine gradient (Hearn and Largier 1997; Smith and Hollibaugh 1997). Broadly, Tomales Bay can be divided into three oceanographic zones: outer-bay, mid-bay, and inner-bay (Smith and Hollibaugh 1997; Kimbro et al. 2009*b*), which are represented in our study as stations 4, 10, and 16 km from the mouth (Fig. 1), respectively.

Seasons in Tomales Bay are defined by predictable associations of water column properties that alter hydrographic and biogeochemical gradients throughout the bay (García-Reyes and Largier 2012). The majority of annual precipitation falls during the wet runoff season (December–February), and the hydrographic signature is most apparent in the inner-bay zone where the inflow of freshwater from the surrounding watershed strongly decreases

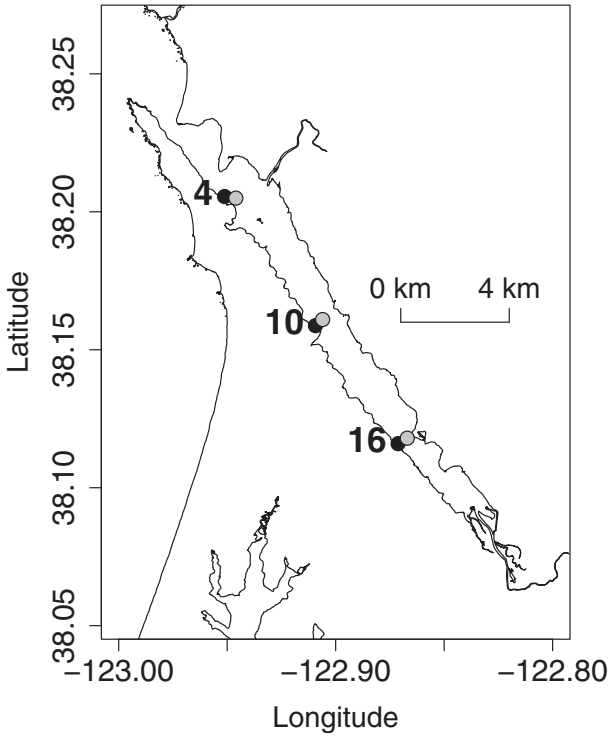

Fig. 1. Map of Tomales Bay, including the oyster deployment stations labeled by distance from the bay mouth in kilometers. Black circles represent the shore sites, while gray circles represent the channel sites.

salinity and alkalinity and increases nutrients while the mid- and outer-bay zones remain tidally influenced (Smith et al. 1991). The upwelling season (April–July) is characterized by strong and persistent wind events, which drive the shoaling of deep water to the surface on the open coast. This cold, hypoxic, nutrient-rich, and corrosive (high-pCO_2) deep water is advected into the outer-bay while high inland temperatures can drive hypersaline conditions in the inner-bay, thus resulting in strong gradients of temperature, salinity, DO, and pH (Smith et al. 1991; Hearn and Largier 1997; Largier et al. 1997). Differences among oceanographic zones are generally least during the relaxation season (August–November) which has few to no precipitation or wind-driven upwelling events and therefore reduced water column mixing. Mid-bay phytoplankton maxima are generally observed during the upwelling and relaxation seasons due to intermediate residence times of tidally advected upwelled nutrients from the open coast (Kimbro et al. 2009*b*). While summer precipitation and winter upwelling can occur, these rare events have little effect on overall bay oceanography and biogeochemistry relative to broad seasonal patterns (Smith et al. 1991). In addition to oceanographic and atmospheric processes, diel cycling of photosynthesis and respiration can strongly impact bay biogeochemistry (Wootton et al. 2008).

Oyster natural history

Olympia oysters (*O. lurida*) are native to western North America from Baja California, Mexico, to Sitka, Alaska (Baker 1995). Spawning occurs late spring to early fall (Baker 1995). Adult

oyster aggregations provide important habitat for diverse benthic algal and invertebrate communities (Kimbro and Grosholz 2006). The current distributions of Olympia oysters in many estuaries, including Tomales Bay, are limited by invasive predators and loss of benthic habitat (Ruesink et al. 2006; Kimbro et al. 2009*b*; Polson and Zacherl 2009).

Pacific oysters (*C. gigas*) are native to the Pacific coast of Asia and are a widespread commercially cultivated species. Pacific oyster mariculture facilities exist at various sites within Tomales Bay. They are not naturalized and spat is imported from outside California.

Water column measurements

At stations 4, 10, and 16 km from the mouth of the bay, we collected water samples with a 2.5-liter Niskin bottle at three depths: channel surface (1 m below the surface), channel bottom (1 m above the benthos), and shore (1 m below surface in water < 3 m deep, within 20 m of the shore, and immediately shoreward of the channel depths). We recorded field measurements of salinity, temperature, potentiometric pH (NBS scale, pH_{NBS}), and DO (saturation and mg L^{-1}) of each Niskin sample, determined using a YSI MPS 556. pH_{NBS} was calibrated using Fisher low ionic-strength buffers and converted to pH total scale (pH_T) using CO2Calcv2.1 (Robbins et al. 2010; constants from Millero 2010). Water from each Niskin sample was collected for laboratory analysis of carbonate system parameters (T_{alk}, DIC, and spectrophotometric pH), DIN (NH_4^+, NO_3^-,NO_2^-), PO_4^{3-}, silicate, and chlorophyll *a* (Chl *a*) (*see* Supporting Information for details on laboratory methods). We calculated DIC and aragonite saturation state (Ω_{arag}) of the water samples with CO2Calc v2.1 (Robbins et al. 2010; constants from Millero 2010) from measured T_{alk} and pH_T. Ω_{arag} is defined as the ratio between in situ dissolved calcium and carbonate ion concentrations to these concentrations at equilibrium with aragonite $\left(\Omega = \frac{([Ca^{2+}])([CO_3^{2-}])}{Ksp}\right)$ (Feely et al. 2004; Fabry et al. 2008). Additionally, at each oceanographic zone in Tomales Bay (*see* Fig. 1) and at most depths (channel surface, channel bottom, shore), we used data from a network of moored sensors that continuously recorded data for several water column parameters, including temperature and conductivity in real time (*see* Supporting Information for details). We wanted to determine the relationship between field temperatures measured during bottle sampling and continuous temperature measurements during this same period.

Laboratory oyster culture

We collected adult Olympia oysters at multiple dates between 01 July 2014 and 24 April 2015 at sites in Tomales Bay and maintained them as broodstock in the UC Davis Bodega Marine Laboratory aquaculture facilities. Oysters were kept at approximately 20°C and fed abundant cultured microalgae to induce spawning. Once larvae were released from the brooding chamber (approximately 10–14 d after fertilization), we allowed oyster larvae to settle on sanded 10 × 10 cm PVC tiles that had collected biofilm in seawater for 24 h. When oysters reached the desired size (~ 0.5 mm), we standardized densities (approximately 20 oysters per tile) to avoid competitive overgrowth. We labeled and photographed each tile 1–3 d prior to each field outplant. For larval oyster outplants, we collected standard densities of larvae after oysters spawned in the laboratory culture tanks and placed them into plastic containers on the day of the outplant, after which they were immediately transported to the field and released in mesh containers (see below).

We cultured Pacific oyster larvae and juveniles using similar methods described above. Larvae were shipped from the Whiskey Creek Shellfish Hatchery, Tillamook, OR (standard importation permit # 2015–3787, CA DFG). Once competent (typically 2–3 weeks), larvae were allowed to settle on 10 × 10 cm PVC tiles.

Both Olympia and Pacific oyster broodstock and settled juveniles were exposed to seasonally variable chemical environments (i.e., DO, pH, T_{alk}) within the aquaculture facilities which could have influenced later performance in the field but was beyond the scope of this experiment.

Juvenile outplant experiments

We randomly assigned tiles with juvenile oysters to one of nine possible locations in Tomales Bay: one of three stations representing the three oceanographic zones (4, 10, or 16 km from the mouth) and one of three depths in the water column (channel surface, channel bottom, or shore) in each zone (Fig. 1). We affixed two PVC pipes with five tiles each to mooring lines at 1–2 m above the substrate for channel bottom depths and 1–2 m below the surface for channel surface depths. Shore sites consisted of two PVC racks with five tiles each that maintained tiles at > 1 m below the surface (*see* Supporting Information for experimental design). All tiles at all depths were submerged even at the lowest tides.

Olympia oyster deployments took place during periods of storm-based runoff (December 2014 and January 2016), upwelling (June 2015 and August 2015), and relaxation (October 2015) while Pacific oyster deployments were limited to runoff (January 2016) and relaxation (October 2015) events. All deployments lasted for approximately 1 month. We recovered all tiles in 1 d and brought them to the lab where we cleaned and photographed each tile within 24 h. We used photos taken both before and after deployment to measure growth and mortality of individual oysters on each tile. We measured the difference in maximal length from the umbo to the outer shell edge, and shell area using image analysis software (IMAGEJ version 1.46; National Institutes of Health, Bethesda, MD, U.S.A.) and mortality by comparing before and after photos for missing oysters. Length and area were highly correlated (Pearson's r = 0.93), so we focused our analyses on length.

Larval outplant experiments

We deployed laboratory-spawned Olympia larvae to the same depths (channel surface, channel bottom, and shore) and stations (4, 10, and 16 km from the mouth) in Tomales Bay during the upwelling season (July 2015) to coincide with the natural timing of oyster spawning and settlement (Pritchard et al. 2015). Larvae were outplanted in PVC pipes with 100 μm mesh secured over each end (*see* Supporting Information for additional description of the enclosure design). Lab trials showed that this created adequate water flow while at the same time retaining all larvae (*see* Becker et al. 2007). We estimated larval density in the laboratory prior to deployment to ensure approximately equal numbers of larvae per enclosure.

Larval deployment lasted 5 d in order to have sufficient time to quantify site-specific growth and survival differences while avoiding the possibility of losing larvae to settlement. Within 24 h of retrieving oyster deployments, we estimated larval mortality by counting the number of empty shells relative to the number of filled shells under a microscope (lens magnification of 10X). We photographed six fields of view per enclosure using a Micropublisher 5.0 RTV digital camera (QImaging) mounted on the microscope and estimated sizes of all larvae in each field of view by measuring the maximum shell length using image analysis software (mean = 20, SD = 12).

Statistical analysis

All analyses were conducted in R (version 3.4.3; R Core Team 2017). We conducted several types of analyses using the environmental data from the discrete samples to determine the influence of temperature, salinity, carbonate chemistry, nutrients, phytoplankton biomass, and other water column variables on oyster performance. We also tested whether the discrete samples effectively captured spatial and seasonal variability in the bay by comparing these data to continuous measurements of temperature and salinity, and a temperature proxy for Ω_{arag}. The discrete samples were a good representation of the continuous data, thus we are confident basing our analyses on these discrete data (*see* Supporting Information for information on continuous monitoring, data analysis, and results).

Water column analysis

We examined patterns of variation among the water column variables to determine the degree of collinearity. These patterns differed dramatically by season, with directions and magnitudes of associations changing between seasons. Using a reduced predictor data set to avoid collinearity (Table 1; *see* Supporting Information for eliminated variables), we conducted ordination analyses to assess the separation of the water column variables among seasons (runoff, upwelling, and relaxation), stations in the three oceanographic zones (outer-, mid-, and inner-bay), and the three depths at each station (channel surface, channel bottom, and shore). Analysis included principal component analysis (PCA) and nonmetric multidimensional scaling (nMDS) of standardized predictor variables (mean = 0; SD = 1) using the *vegan* package (Oksanen et al. 2018). We examined each season separately to evaluate the Euclidean separation of water column variables by station and depth using permutational multivariate ANOVA with Euclidean distance matrices. For these analyses, we categorized the discrete water samples into seasons and treated all samples across stations and depths as independent. We examined Chl *a* from the bottle samples using ANOVA to explicitly test for spatial and seasonal variation in phytoplankton biomass,

Table 1. Loadings for the first (PC1) and second (PC2) principal components axes for water column properties, separated by season.

	Runoff	Upwelling		Relaxation	
	PC1	PC2	PC1	PC2	PC1	PC2
Chl *a* (mg m^{-3})	1.06	0.43	0.55	−0.01	−0.54	−1.37
DO (% air saturation)	−0.27	−0.60	0.90	0.43	−0.79	0.56
NH_4^+ (μmol L^{-1})	−1.09	0.22	−0.37	0.37	1.44	−0.44
NO_2 (μmol L^{-1})	0.87	−0.23	−0.89	0.19	−0.63	−0.70
NO_3^- (μmol L^{-1})	1.09	−0.15	−1.08	0.46	0.84	−0.15
pCO_2 (μatm)	−0.97	0.28	−1.21	−0.53	1.39	−0.62
pH_T	0.04	−0.60	0.97	0.07	0.09	1.11
PO_4^{3-} (μmol L^{-1})	1.09	0.11	−0.43	−1.08	1.54	−0.25
Salinity (PSU)	−1.16	0.10	0.29	−0.22	1.57	0.35
Silicate (μmol L^{-1})	1.02	0.29	−0.12	−0.62	−0.50	−1.40
T_{alk} (μmol kg^{-1})	−1.17	0.08	0.33	−1.25	1.48	−0.01
tCO_2 (μmol kg^{-1})	0.62	0.23	−0.60	−1.15	1.15	−0.77
Temperature (°C)	0.04	−1.10	0.60	−1.15	1.35	0.60
Ω_{arag}	0.16	−0.24	1.29	−0.28	0.06	0.12
Variance explained	0.51	0.21	0.3	0.24	0.45	0.21

including the presence of the persistent mid-bay phytoplankton maximum (Kimbro et al. 2009*b*).

Oyster growth and survival analysis

We used linear mixed-effects models with the *lme4* and *lmerTest* packages in R (Bates et al. 2015; Kuznetsova et al. 2017) and generalized linear models to understand the effects of water column variation on juvenile and larval oyster growth and survival. We conducted separate analyses for each season (upwelling, runoff, and relaxation). Experimental outplants included growth and survival of Olympia oysters in all seasons; growth and survival of Pacific oysters in the runoff and relaxation seasons; and growth and survival of larval Olympia oysters in the upwelling season. For all analyses, we examined residual structure and log-transformed growth data when necessary to meet assumptions of the analyses (*see* Supporting Information for additional details). We conducted post hoc pairwise comparisons using Tukey tests in the *lsmeans* package (Lenth 2016). In addition to season-specific linear models, we also compared mean growth values across species and seasons using Welch's *t*-test.

Using two sets of linear mixed-effects models per season, we tested the effects of water column variation on oyster growth, defined as $\left(\frac{\text{final length} - \text{initial length}}{\text{initial length}}\right)$*days deployed^{-1}, and survival. We fit a separate model for each season. The first set of models tested the interaction of stations (4, 10, and 16 km from the mouth) and depth within each station (channel surface, channel bottom, shore) on juvenile Olympia and Pacific oyster growth and survival, and larval Olympia size and survival. We assumed that individual oyster responses could be correlated on the same settlement tile and therefore included tile as a random effect in all of our models of individual oyster responses. In model runs where there was no significant interaction between station and depth, we removed the interaction term and reran the model.

The second set of models determined the influence of water chemistry on oyster growth and survival. For these analyses, we used the first and second principal components from our water column analysis (see above) for each season as a predictor variable. We analyzed whether these principal components had a direct effect on individual oyster growth and survival, and included a random effect of settlement tile to account for any influence of settlement tile on growth.

Results

Water column analysis

Water column parameters and their associations differed strongly by season (Tables 1, 2) and location in the bay, as seen in the nMDS plots (Fig. 2), consistent with past studies on Tomales Bay (*see* "Site description" section). Permutational ANOVA results showed significant differentiation among stations during runoff season ($F_{2,28}$ = 2.8, R^2 = 0.16, p = 0.01) with no significant variation across depths (Table 2). The most important variables distinguishing runoff season water column properties were consistent with riverine derived variables, including temperature, salinity, nutrients (PO_4^{3-}, NH_4^+, NO_3^-, NO_2), silicate, Chl *a*, and carbonate chemistry (T_{alk} and pCO_2) (runoff-season PC1 and PC2; *see* Table 1). Minimum salinity recorded from bottle samples during the runoff season were 13.1 PSU and 17.4 PSU in the mid- and inner-bay, respectively. Water column properties also differed significantly by station ($F_{2,56}$ = 7.9, R^2 = 0.22, p = 0.001) for upwelling season with no significant effect of depth (shore, channel surface, channel bottom) (Table 2). Variation in upwelling-season water column properties was most driven by temperature, DO, carbonate chemistry (pH_T, T_{alk}, Ω_{arag}, tCO_2, pCO_2), and nutrients (PO_4^{3-}, NO_3^-, NO_2) (upwelling-season PC1 and PC2; *see* Table 1), consistent with the chemical signature of upwelled waters (i.e., low pH, low DO, and high DIN). Water column properties differed significantly by depth ($F_{2,102}$ = 2.4, R^2 = 0.03, p = 0.02) and station

Table 2. Analysis of water column parameters (*see* Table 4) by station and depth for each season using permutational multivariate ANOVA.

Season		df	Sums of squares	Mean squares	*F*	R^2	*p*
Upwelling	Station	2	170.44	85.22	7.93	0.22	0.001
	Depth	2	11.06	5.53	0.51	0.01	0.93
	Residuals	56	601.50	10.74	—	0.77	—
	Total	60	783.00	—	—	—	—
Runoff	Station	2	66.91	33.45	2.90	0.16	0.01
	Depth	2	37.95	18.98	1.64	0.09	0.09
	Residuals	28	323.14	11.54	—	0.76	—
	Total	32	428.00	—	—	—	—
Relaxation	Station	2	546.58	273.29	36.06	0.40	0.001
	Depth	2	36.34	18.17	2.40	0.03	0.02
	Residuals	102	773.08	7.58	—	0.57	—
	Total	106	1356.00	—	—	—	—

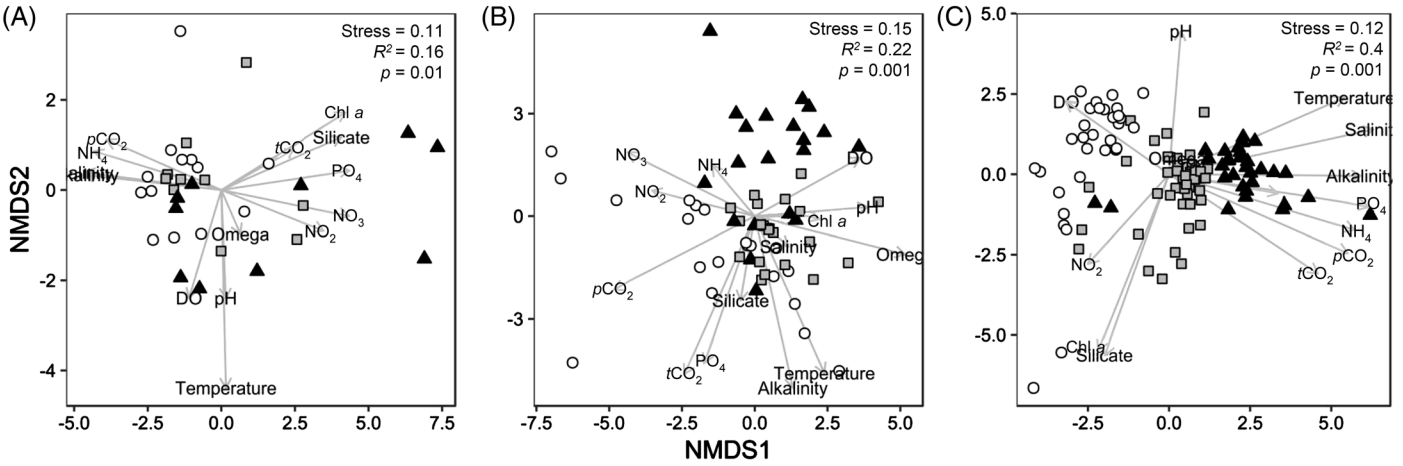

Fig. 2. Nonmetric multidimensional scaling plots of z-transformed environmental parameters across the estuarine gradient during the (**A**) runoff, (**B**) upwelling, and (**C**) relaxation seasons using a Euclidean dissimilarity index. Shapes indicate sampling stations: 4 km (circle), 10 km (triangle), and 16 km (square) from the mouth of the bay. Stress in two-dimensions and statistical output (R^2 and p) from permutational multivariate ANOVA are noted for the analysis of each respective season.

($F_{2,102}$ = 36, R^2 = 0.4, p = 0.001) during the relaxation season (Table 2), suggesting depth stratification. Differences were driven by temperature, salinity, carbonate chemistry (T_{alk}, pH_T, tCO_2, pCO_2), Chl *a*, silicate, and nutrients (NH_4^+, PO_4^{3-}) (relaxation-season PC1 and PC2; *see* Table 1).

Temperature recorded during event-driven bottle sampling was positively and strongly correlated with the mean of the continuous temperature during oyster outplants (Pearson's r = 0.96, t = 16.9, df = 25, $p < 0.001$). The magnitude of site-level differences in temperature differed by season, with the strongest difference in the summer (Supporting Information Fig. S2). Therefore, while the event-driven bottle samples used for our analysis did not capture daily variability, they effectively captured the average condition experienced by the oysters and the seasonal and spatial variation in water column properties.

Chl *a* concentrations during the upwelling season showed nonsignificant trends toward higher Chl *a* levels in our bottle samples from the mid-bay compared to the inner-bay ($F_{2,37}$ = 2.9, p = 0.06). We did not observe differences in Chl *a* concentrations throughout the bay in the relaxation or runoff seasons.

Oyster growth and survival

Juvenile Olympia oyster growth during the runoff season was significantly lower throughout the bay compared to upwelling and relaxation seasons ($F_{2,2214}$ = 1411, $p < 0.001$) with only slight differences across stations and depths (Fig. 3). Growth was significantly lower in both the outer-bay channel surface (t = 3.65, df = 64.8, p = 0.01) and inner-bay channel bottom sites (t = −3.78, df = 63.8, p = 0.01) compared with the mid-bay shore site where we observed highest growth (*see* Supporting Information Table S1 for model output and pairwise comparisons based on Tukey tests). The first PC axis was a significant negative predictor of juvenile Olympia oyster growth (t = −4.55, df = 54.3, $p < 0.001$; *see* Table 3A). Juvenile Olympia oyster survival was high across all sites (Fig. 3). Survival was lowest at inner-bay channel sites ($z \leq -4.15$, $p < 0.001$) and the outer-bay channel bottom ($z \leq -4.2$, $p < 0.001$), and highest at the mid-bay and shore sites ($z \geq 3.8$,

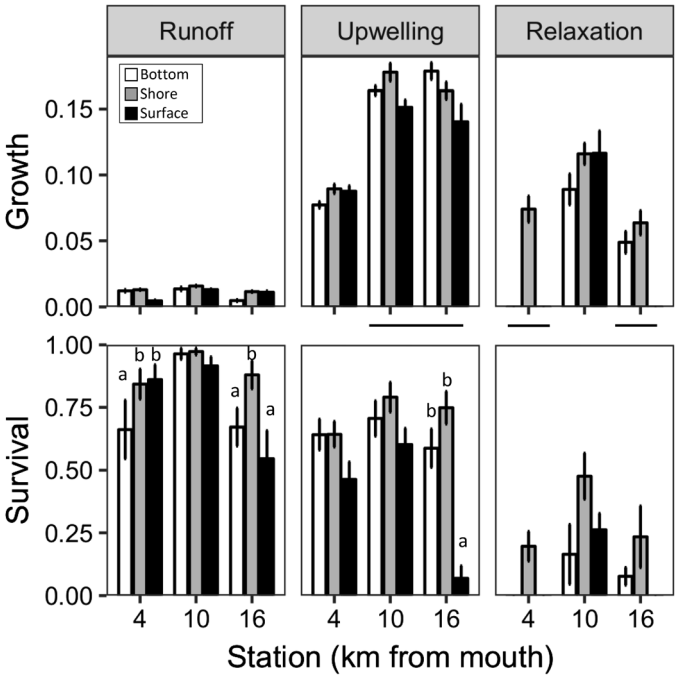

Fig. 3. Proportional daily growth (top) and proportional survival (bottom) of juvenile Olympia oysters during the runoff, upwelling, and relaxation seasons. Bar height and errors represent mean and standard error, respectively. Bar colors represent the experimental depths: channel bottom (white), shore (gray), and channel surface (black). For seasons with a significant interaction of station and depth, letters (a and b) above the bars indicate significant differences ($p < 0.05$) among depths within a given station. For seasons with no significant interaction between station and depth, stations indicated by a bar below the station label on the *X* axis are significantly different from stations without underline bars.

Table 3. Results of linear mixed effects models for log-transformed growth of (A) Olympia oysters and (B) Pacific oysters by principal components axes 1 and 2 analyzed for each season.

Season	Main effects	Estimate	SE	df	*t*	*p*
(A)						
Runoff	PC1	−0.01	0.00	54.29	−4.55	< 0.001
	PC2	−0.04	0.02	49.90	−1.61	0.12
Upwelling	PC1	0.09	0.01	120.29	7.90	< 0.001
	PC2	−0.02	0.01	98.29	−3.51	< 0.001
Relaxation	PC1	−0.02	0.02	32.08	−1.04	0.31
	PC2	0.07	0.06	30.53	1.13	0.27
(B)						
Runoff	PC1	0.04	0.01	20.14	2.51	0.02
	PC2	0.08	0.08	11.32	1.07	0.31
Relaxation	PC1	−0.14	0.07	13.10	−1.85	0.09
	PC2	0.45	0.34	15.87	1.33	0.20

$p \leq 0.004$; *see* Supporting Information Table S2 for model output and pairwise comparisons). As with growth, the first PC axis was a significant negative predictor of Olympia oyster survival ($z = -2.13$, $p = 0.03$). Therefore, low growth and low survival of juvenile Olympia oysters during the runoff season were associated with water masses that were less saline, less alkaline, and high in nutrients and Chl *a*, consistent with freshwater runoff driving reduced oyster growth and survival in the inner-bay.

Juvenile Pacific oyster growth during runoff season was significantly greater than Olympia growth ($t = 5.7$, df = 88, $p < 0.001$; *see* Table 4). Juvenile Pacific oyster growth mirrored patterns observed in Olympia oysters with inner-bay channel bottom growth significantly lower than growth at shore sites ($t \leq -3.35$, df = 76, $p \leq 0.03$; *see* Fig. 4, Supporting Information Table S3). However, the first PC axis was a significant positive predictor of juvenile Pacific growth during runoff season ($t = 2.5$, df = 20, $p = 0.02$; *see* Table 3B). Juvenile Pacific survival was significantly lower at the inner-bay channel surface site compared to sites with the highest observed survival: mid- and inner-bay shore and outer-bay channel bottom ($z \leq -3.51$, $p \leq 0.04$; *see* Fig. 4, Supporting Information Table S4) and the first PC axis was a significant negative predictor of juvenile Pacific survival during runoff season ($z = -2.45$, $p = 0.01$). This suggests that, like Olympia oysters, Pacific oyster survival during the runoff season was similarly negatively affected by exposure to freshwater runoff while juvenile Pacific oyster growth was positively associated with freshwater runoff.

Our across-season analysis indicated that Olympia juvenile growth was greatest during the upwelling season ($F_{2,2214} = 1411$, $p < 0.001$; *see* Table 4). However, our within-season analysis indicated that most of that growth is driven by oysters growing in the warmer inner-bay sites. Growth was significantly lower in the outer bay compared to mid- and inner-bay sites ($t \geq 8.0$, df = 100,

Table 4. Summary statistics of water column parameters by season showing mean, SD, and *n* of water column parameter measurements across stations, depths, and sampling dates within each season (*n* is the number of measurements contributing to the mean and SD).

	Runoff			Upwelling			Relaxation		
Season	**Mean**	**SD**	***n***	**Mean**	**SD**	***n***	**Mean**	**SD**	***n***
Chl *a* (mg m^{-3})	1.8	1.1	32	5.4	4.1	40	6.0	5.0	23
DO (% air saturation)	109.7	22.1	24	104.6	9.1	55	96.9	9.1	86
NH_4^+ (μmol L^{-1})	3.8	1.7	32	1.6	2.5	55	1.3	0.9	107
NO_2 (μmol L^{-1})	0.6	0.3	32	0.2	0.1	55	0.2	0.1	107
NO_3^- (μmol L^{-1})	7.8	6.4	32	2.1	4.7	55	0.6	1.3	107
pCO_2 (μatm)	573.6	117.0	32	586.1	141.2	61	589.3	118.7	100
pH_T	7.8	0.1	32	7.9	0.2	61	8.0	0.2	106
PO_4^{3-} (μmol L^{-1})	1.6	0.3	32	2.0	0.7	55	2.6	1.1	107
Salinity (PSU)	29.1	3.5	33	33.4	1.2	61	34.1	0.7	107
Silicate (μmol L^{-1})	28.8	15.3	32	25.8	11.1	55	35.2	16.8	107
T_{alk} (μmol kg^{-1})	2131.3	119.0	32	2317.6	68.0	61	2354.0	97.1	106
tCO_2 (μmol kg^{-1})	2008.8	94.4	32	2136.1	67.5	61	2155.5	93.1	100
Temperature (°C)	13.4	1.2	33	17.4	2.9	61	18.9	2.1	107
Ω_{arag}	1.6	0.4	32	2.2	0.5	61	2.3	0.3	100
Olympia daily growth	0.013	0.01	834	0.138	0.08	1248	0.096	0.06	135
Olympia % survival	0.82	0.3	89	0.62	0.3	136	0.28	0.2	34
Pacific daily growth	0.024	0.02	85	—	—	—	0.091	0.04	23
Pacific % survival	0.46	0.3	40	—	—	—	0.09	0.1	39
Olympia larval growth	—	—	—	0.167	0.01	341	—	—	—
Olympia larval % survival	—	—	—	0.37	0.3	106	—	—	—

$p < 0.001$; *see* Fig. 3, Supporting Information Table S1), consistent with bay locations more influenced by advected upwelled water from the open coast (Fig. 2). The first PC axis was a significant positive predictor of growth ($t = 7.9$, df = 120, $p < 0.001$) while the second PC axis was a significant negative predictor of growth ($t = -3.5$, df = 98, $p < 0.001$; *see* Table 3A), suggesting that higher juvenile Olympia oyster growth during upwelling season was associated with water masses in the mid- and inner-bay that were warmer, more alkaline, and had high DO, pH, Ω_{arag}, and low pCO_2 (Table 1). In other words, oysters that were not directly exposed to upwelled waters such as those in the lower bay grew more during this season. Survival was lowest at the channel surface in the inner-bay ($z \geq 4.29$, $p < 0.001$; *see* Fig. 3, Supporting Information Table S2) and was not significantly predicted by either the first or second PC axes.

Olympia larval growth during upwelling season (August 2015 outplant) showed similar patterns as juvenile growth with lowest values observed in the outer-bay channel bottom compared to mid-bay channel surface site ($t \leq -3.59$, $p \leq 0.01$; *see* Fig. 5, Supporting Information Table S5). The first and second PC axes were not significant predictors of growth. Larval survival was highest at outer-bay shore and mid-bay channel bottom sites ($z \geq 3.7$, $p \leq 0.007$) and lowest at outer-bay and inner-bay channel sites ($z \leq 3.7$, $p \leq 0.007$; *see* Fig. 5, Supporting Information Table S6).

The first PC axis was a significant negative predictor of larval survival ($z = -3.58$, $p < 0.001$) suggesting that low larval survival during upwelling season was associated with water masses that had high nutrient concentrations, low DO, high pCO_2, and low Ω_{arag}, consistent with upwelled water leading to greater larval mortalities.

Overall growth of juvenile Olympia oysters during the relaxation season was significantly higher than the runoff season and lower than the upwelling season ($F_{2,2214} = 1411$, $p < 0.001$; *see* Table 4). Within-season analysis indicated that mid-bay growth was higher than in the inner-bay ($t = 2.9$, df = 14, $p = 0.02$; *see* Fig. 3, Supporting Information Table S1), and neither the first nor second PC axis was a significant predictor of Olympia growth during the relaxation season (Table 3A). Proportional survival of juvenile Olympia oysters was low throughout the bay with no significant differences in survival across sites (Fig. 3, Supporting Information Table S2). The first PC axis was a significant negative predictor of Olympia oyster survival ($z = -2.37$, $p = 0.02$) and the second PC axis was a significant positive predictor ($z = 3.47$, $p < 0.001$). This suggests that higher Olympia oyster survival during the relaxation season was associated with water masses that had higher Chl *a* and nutrient concentrations, pCO_2, temperature, salinity, silicate, and alkalinity, and lower pH. Juvenile Pacific oyster growth did

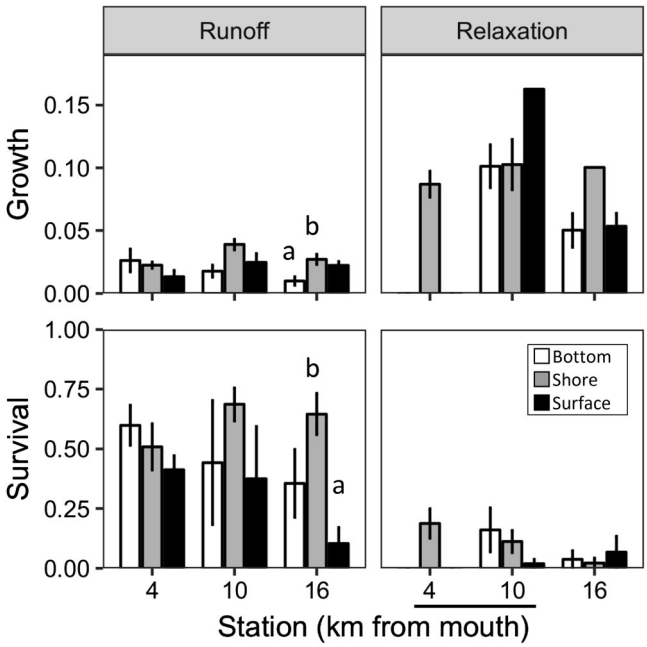

Fig. 4. Proportional daily growth (top) and proportional survival (bottom) of juvenile Pacific oysters during the runoff and relaxation seasons. Bar height and errors represent mean and standard error, respectively. Bar colors represent the experimental depths, including channel bottom (white), shore (gray), and channel surface (black). For seasons with a significant interaction of station and depth, letters (a and b) above the bars indicate significant differences ($p < 0.05$) among depths within a given station. For seasons with no significant interaction between station and depth, stations indicated by a bar below the station label on the *X* axis are significantly different from stations without underline bars.

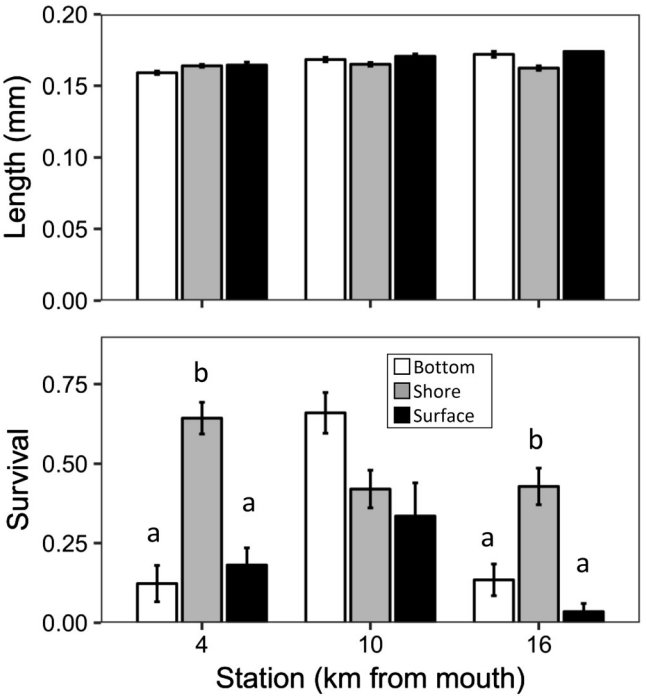

Fig. 5. Length in millimeters (top) and proportional survival (bottom) of larval Olympia oysters during the upwelling season. Bar height and lines represent mean and standard error, respectively. Bar colors represent the experimental depths, including channel bottom (white), shore (gray), and channel surface (black). Letters (a and b) above the bars indicate significant differences ($p < 0.05$) among depths within a given station.

not differ significantly from Olympia oyster growth, with no significant difference in growth among sites (Fig. 4, Supporting Information Table S3) and no significant effect of PC loadings on growth (Table 3B). Juvenile Pacific oyster survival was significantly lower in the inner bay compared to the mid-bay (z = 3.3, p = 0.002; *see* Fig. 4, Supporting Information Table S4) with no significant effect of PC loading.

Discussion

This study clearly demonstrates that seasonal processes such as coastal upwelling and river input during floods can significantly influence the water chemistry of the Tomales Bay estuary and likely many similar estuaries in regions dominated by Mediterranean climates or strong coastal upwelling (Largier et al. 1997; Hickey and Banas 2003). We have linked this spatial and temporal variation in water column chemistry to the growth and survival of key bivalve species in this system: the ecologically important Olympia oyster, and the commercially important Pacific oyster. In particular, our results demonstrate the lethal and sublethal impacts of changes in water chemistry and hydrography associated with both upwelling and terrestrial river run-off. Since climate models project changes in the frequency and intensity of wind-driven summer upwelling and winter rainfall events (Cayan et al. 2008; Sydeman et al. 2014), these results will enable more quantitative estimates of how future changes will impact the growth and survival of these species.

During the winter runoff season, cold temperatures and low phytoplankton levels corresponded with low oyster growth throughout the bay. The lowest rates of growth and survival for both Olympia and Pacific juvenile oysters were observed in regions most impacted by freshwater inflow, though based on PC analysis, Pacific juveniles are less susceptible than Olympia juveniles to runoff events. Our runoff season observations are likely an underestimate of riverine impacts on bay hydrography and oyster performance as our study took place during the late stages of a record-breaking California drought (Robeson 2015; Supporting Information). However, it is notable that even though salinity never reached lethal low levels as identified in laboratory experiments (Wiltshire 2007; Cheng et al. 2015; Gray and Langdon 2018), oyster performance in the inner bay was still significantly negatively impacted. Pacific and Olympia oysters respond to low salinity conditions by reducing pumping activity, leading to decreased food consumption and gas exchange and this effect is observed even at moderately reduced salinity levels (< 20 PSU) when measured over short (1 d) time series (Gray and Langdon 2018). Our results demonstrate the lethal and sublethal effects of chronic (1 month) exposure to moderate terrestrial runoff which includes reduced salinity in addition to low alkalinity and high pCO_2.

During the spring/summer upwelling season, oyster performance reflected the competing stressors of corrosive yet nutrient-rich upwelled water and high water temperatures, conditions that are also observed in outer coast estuaries in the Pacific Northwest (Hickey and Banas 2003). While growth during this season was highest overall, likely due to the combined effects of warmer average temperatures and greater food availability (Kimbro et al. 2009*b*), we still observed the detrimental effects of upwelled water and stressfully high temperatures on Olympia larval and juvenile oysters. As Olympia oysters spawn during the late spring to early fall (Baker 1995), larval oysters were outplanted during the upwelling season to reflect realistic exposure to environmental conditions. Reduced larval growth and survival in the outer-bay where larvae were exposed to undersaturated water with respect to aragonite is consistent with some laboratory findings (Hettinger et al. 2012, Hettinger et al. 2013, but see Waldbusser et al. 2016). Research in controlled settings also suggests that this exposure to corrosive water during early life stages has negative carry-over effects at later juvenile stages, which could influence later ecosystem functioning (Hettinger et al. 2012). Likewise, Cheng et al. (2017) demonstrated reduced oyster performance under high temperatures in reduced food conditions, as is often observed in the inner bay during upwelling season (Kimbro et al. 2009*b*). Our PC analysis also suggests that oyster juvenile growth and larval survival was impacted by DO concentrations which were low in the outer- and inner-bay due to upwelling and reduced mixing, respectively. Together, the results from the upwelling season highlight the importance of considering multiple stressors and spatial refugia when estimating the response of organisms to environmental change.

During the relaxation season, the water column was characterized by reduced water column mixing and resultant stratification due to the lack of stressful inputs of freshwater or corrosive upwelled water (García-Reyes and Largier 2012). Despite these relatively stable oceanographic conditions, survival rates for both oyster species during this period were generally lower compared to the other seasons. While we did not observe a significant mid-bay phytoplankton peak (Kimbro et al. 2009*b*), we did find significantly higher mid-bay Olympia oyster growth and trends toward higher Pacific oyster growth suggesting some mid-bay benefit for oyster growth, as well as higher oyster survival associated with higher Chl *a* concentrations.

Our results reflect the direct effects of abiotic water column properties on oyster performance. We found no indication of predation pressure such as shell holes created by oyster drills and no predators were present on recovered plates. While there were variable levels of fouling on plates (e.g., tunicates and bryozoans), we observed no patterns between oyster survival or growth and fouling. Additionally, disease prevalence among Olympia oysters in Tomales Bay is exceedingly low and disease-related mortalities within Pacific oyster farms occur during upwelling season when we did not outplant Pacific oysters (Moore et al. 2011). Densities of both oyster predators and fouling organisms are known to increase along gradients of temperature and salinity on natural substrates and may represent seasonal and spatial stressors that were not included in this study (Kimbro et al. 2009*a*; Osman et al. 2010; Chang et al. 2018).

Future projections of regional climate change suggest several changes that will be intensified in the future. The frequency and intensity of upwelling events is likely to increase as the result of increased wind stress in the central region of the California coast (García-Reyes and Largier 2010). This increased upwelling will likely increase the presence of hypoxic and barely saturated or undersaturated waters with respect to Ω_{arag} that could be tidally advected into coastal estuaries like Tomales Bay (Feely et al. 2010). Accompanying this increase in wind-driven upwelling is a projected increase in inland temperatures leading to higher inner-bay temperatures and hypersaline conditions (Cayan et al. 2008). Given the demonstrated stressful nature of both corrosive waters and exceedingly high temperatures, the mid-bay refuge for Olympia and Pacific oysters observed in this study may shrink, with potentially severe ecosystem and economic consequences.

Increased interannual variation in precipitation is also projected in the future (Cayan et al. 2008). The subsequent inflow of freshwater from the surrounding watershed into the bay could increase the variability of salinity and Ω_{arag} during the wet season, including increasing the frequency and intensity of pulse run-off events. These extreme run-off events have been linked to atmospheric rivers in nearby San Francisco Bay, and result in mass oyster mortality events (Cheng et al. 2016). We observed reduced Olympia and Pacific oyster performance in regions impacted by moderate levels of riverine runoff; therefore, increased frequency or duration of high precipitation events could severely negatively impact native and commercial oyster populations. Additionally, changes to both upwelling and runoff seasonality will likely impact the duration and characteristics of the relaxation season, a period of general atmospheric stability that coincides with Olympia oyster spawning (Pritchard et al. 2015). As demonstrated in this study, Olympia oyster larvae are vulnerable to exposure to upwelled waters and high temperature inner-bay conditions, both of which may occur later in the season in the future (Cayan et al. 2008; García-Reyes and Largier 2010). These conditions are likely responsible for the strong interannual variation in recruitment seen in Olympia oysters at this site (Kimbro et al. 2018) and projected climate change could increase recruitment variability in the future.

By linking precipitation and upwelling events with spatial and temporal variation in growth and survival of oysters, we provide the basis for understanding how the population dynamics of two important species in western estuaries are likely to be affected by future climate change. Current thinking about climate change impacts in habitats like coastal estuaries suggest that the most important impacts of climate change are likely to be experienced by the increasing frequency and magnitude of extreme climate events. By quantifying the changes in water column properties due to episodes of dry season upwelling and wet season river inflows and their impacts on oyster demography, we now have substantially extended our ability to predict future changes in oyster demography under increasingly extreme climatic events in this region.

References

Andersson, A., et al. 2015. Understanding ocean acidification impacts on organismal to ecological scales. Oceanography **25**: 16–27. doi:10.5670/oceanog.2015.27

Baker, P. 1995. Review of ecology and fishery of the olympia oyster, *Ostrea lurida* with annotated bibliography. J. Shellfish Res. **14**: 501–518.

Banas, N. S., B. M. Hickey, J. A. Newton, and J. L. Ruesink. 2007. Tidal exchange, bivalve grazing, and patterns of primary production in Willapa Bay, Washington, USA. Mar. Ecol. Prog. Ser. **341**: 123–139. doi:10.3354/meps341123

Barton, A., B. Hales, G. G. Waldbusser, C. Langdon, and R. A. Feely. 2012. The Pacific oyster, *Crassostrea gigas*, shows negative correlation to naturally elevated carbon dioxide levels: Implications for near-term ocean acidification effects. Limnol. Oceanogr. **57**: 698–710. doi:10.4319/lo.2012.57.3.0698

Bates, D., M. Maechler, B. Bolker, and S. Walker. 2015. Fitting linear mixed-effects models using lme4. J. Stat. Softw. **67**: 1–48. doi:10.18637/jss.v067.i01

Becker, B. J., L. A. Levin, F. J. Fodrie, and P. A. McMillan. 2007. Complex larval connectivity patterns among marine invertebrate populations. Proc. Natl. Acad. Sci. USA **104**: 3267–3272. doi:10.1073/pnas.0611651104

Breitburg, D. L., and others. 2015. And on top of all that…: Coping with ocean acidification in the midst of many stressors. Oceanography **28**: 48–61. doi:10.5670/oceanog.2015.31

Cayan, D. R., E. P. Maurer, M. D. Dettinger, M. Tyree, and K. Hayhoe. 2008. Climate change scenarios for the California region. Clim. Change **87**: 21–42. doi:10.1007/s10584-007-9377-6

Chang, A. L., C. W. Brown, J. A. Crooks, and G. M. Ruiz. 2018. Dry and wet periods drive rapid shifts in community assembly in an estuarine ecosystem. Glob. Chang. Biol. **24**: e627–e642. doi:10.1111/gcb.13972

Cheng, B. S., and others. 2015. Testing local and global stressor impacts on a coastal foundation species using an ecologically realistic framework. Glob. Chang. Biol. **21**: 2488–2499. doi:10.1111/gcb.12895

Cheng, B. S., A. L. Chang, A. Deck, and M. C. Ferner. 2016. Atmospheric rivers and the mass mortality of wild oysters: Insight into an extreme future? Proc. Biol. Sci. **283**: 20161462. doi:10.1098/rspb.2016.1462

Cheng, B. S., L. M. Komoroske, and E. D. Grosholz. 2017. Trophic sensitivity of invasive predator and native prey interactions: integrating environmental context and climate change. Funct. Ecol. **31**: 642–652. doi:10.1111/1365-2435.12759

Fabry, V. J., B. A. Seibel, R. A. Feely, and J. C. Orr. 2008. Impacts of ocean acidification on marine fauna and

ecosystem processes. ICES J. Mar. Sci. **65**: 414–432. doi:10.1093/icesjms/fsn048

Feely, R. A., C. L. Sabine, K. Lee, W. Berelson, J. Kleypas, V. J. Fabry, and F. J. Millero. 2004. Impact of anthropogenic CO_2 on the $CaCO_3$ system in the oceans. Science **305**: 362–366. doi:10.1126/science.1097329

Feely, R. A., C. L. Sabine, J. M. Hernandez-Ayon, D. Ianson, and B. Hales. 2008. Evidence for upwelling of corrosive "acidified" water onto the continental shelf. Science **320**: 1490–1492. doi:10.1126/science.1155676

Feely, R. A., S. R. Alin, J. Newton, C. L. Sabine, M. Warner, A. Devol, C. Krembs, and C. Maloy. 2010. The combined effects of ocean acidification, mixing, and respiration on pH and carbonate saturation in an urbanized estuary. Estuar. Coast. Shelf Sci. **88**: 442–449. doi:10.1016/j.ecss.2010.05.004

García-Reyes, M., and J. Largier. 2010. Observations of increased wind-driven coastal upwelling off central California. J. Geophys. Res. Oceans **115**: C04011. doi:10.1029/2009JC005576

García-Reyes, M., and J. L. Largier. 2012. Seasonality of coastal upwelling off central and northern California: New insights, including temporal and spatial variability. J. Geophys. Res. Oceans **117**: C03028. doi:10.1029/2011JC007629

Gray, M. W., and C. J. Langdon. 2018. Ecophysiology of the Olympia Oyster, *Ostrea lurida*, and Pacific Oyster, *Crassostrea gigas*. Estuaries Coast. **41**: 521–535. doi:10.1007/s12237-017-0273-7

Hearn, C. J., and J. L. Largier. 1997. The summer buoyancy dynamics of a shallow Mediterranean estuary and some effects of changing bathymetry: Tomales Bay, California. Estuar. Coast. Shelf Sci. **45**: 497–506. doi:10.1006/ecss.1996.0197

Herbert, R. J. H., J. Humphreys, Clare. J. Davies, C. Roberts, S. Fletcher, and Tasman. P. Crowe. 2016. Ecological impacts of non-native Pacific oysters (Crassostrea gigas) and management measures for protected areas in Europe. Biodivers. Conserv. **25**: 2835–2865. doi:10.1007/s10531-016-1209-4

Hettinger, A., et al. 2012. Persistent carry-over effects of planktonic exposure to ocean acidification in the Olympia oyster. Ecology **93**: 2758–2768. doi:10.1890/12-0567.1

Hettinger, A., E. Sanford, T. M. Hill, J. D. Hosfelt, A. D. Russell, and B. Gaylord. 2013. The influence of food supply on the response of Olympia oyster larvae to ocean acidification. Biogeosciences **10**: 6629–6638. doi:10.5194/bg-10-6629-2013

Hickey, B. M., and N. S. Banas. 2003. Oceanography of the U.S. Pacific Northwest Coastal Ocean and estuaries with application to coastal ecology. Estuaries **26**: 1010–1031. doi:10.1007/BF02803360

Hirahara, S., M. Ishii, and Y. Fukuda. 2014. Centennial-scale sea surface temperature analysis and its uncertainty. J. Clim. **27**: 57–75. doi:10.1175/JCLI-D-12-00837.1

Kimbro, D. L., and E. D. Grosholz. 2006. Disturbance influences oyster community richness and evenness, but not diversity. Ecology **87**: 2378–2388. doi:10.1890/0012-9658(2006)87[2378:DIOCRA]2.0.CO;2

Kimbro, D. L., E. D. Grosholz, A. J. Baukus, N. J. Nesbitt, N. M. Travis, S. Attoe, and C. Coleman-Hulbert. 2009*a*. Invasive species cause large-scale loss of native California oyster habitat by disrupting trophic cascades. Oecologia **160**: 563–575. doi:10.1007/s00442-009-1322-0

Kimbro, D. L., J. Largier, and E. D. Grosholz. 2009*b*. Coastal oceanographic processes influence the growth and size of a key estuarine species, the Olympia oyster. Limnol. Oceanogr. **54**: 1425–1437. doi:10.4319/lo.2009.54.5.1425

Kimbro, D. L., J. W. White, and E. D. Grosholz. 2018. The dynamics of open populations: Integration of top–down, bottom–up and supply–side influences on intertidal oysters. Oikos **128**: 584–595. doi:10.1111/oik.05892

Kuznetsova, A., P. B. Brockhoff, and R. H. B. Christensen. 2017. lmerTest package: Tests in linear mixed effects models. J. Stat. Softw. **82**: 1–26. doi:10.18637/jss.v082.i13

Largier, J. L., J. T. Hollibaugh, and S. V. Smith. 1997. Seasonally hypersaline estuaries in Mediterranean-climate regions. Estuar. Coast. Shelf Sci. **45**: 789–797. doi:10.1006/ecss.1997.0279

Lenth, R. V. 2016. Least-squares means: The R package lsmeans. J. Stat. Softw. **69**: 1–33. doi:10.18637/jss.v069.i01

Millero, F. J. 2010. Carbonate constants for estuarine waters. Mar. Freshw. Res. **61**: 139–142. doi:10.1071/MF09254

Moore, J. D., C. I. Juhasz, and T. T. Robbins. 2011. A histopathology survey of California oysters. Calif Fish Game **97**: 68–83.

Oksanen, J., and others. 2018. Vegan: Community ecology package. R package version 2.4-6. Available from https://CRAN.R-project.org/package=vegan Last accessed 03 May 2019.

Osman, R., P. Munguia, R. Whitlatch, R. Zajac, and J. Hamilton. 2010. Thresholds and multiple community states in marine fouling communities: Integrating natural history with management strategies. Mar. Ecol. Prog. Ser. **413**: 277–289. doi:10.3354/meps08673

Polson, M. P., and D. C. Zacherl. 2009. Geographic distribution and intertidal population status for the Olympia oyster, *Ostrea lurida* Carpenter 1864, from Alaska to Baja. J. Shellfish Res. **28**: 69–77. doi:10.2983/035.028.0113

Pritchard, C., A. Shanks, R. Rimler, M. Oates, and S. Rumrill. 2015. The Olympia oyster *Ostrea lurida*: Recent advances in natural history, ecology, and restoration. J. Shellfish Res. **34**: 259–271. doi:10.2983/035.034.0207

R Core Team. 2017. R: A language and environment for statistical computing. R Foundation for Statistical Computing. Available from https://www.R-project.org/ Last accessed 03 May 2019.

Robbins, L. L., M. E. Hansen, J. A. Kleypas, and S. C. Meylan. 2010. CO2calc:a user-friendly seawater carbon calculator for Win-dows, Max OS X, and iOS (iPhone), U.S. Geological Sur-vey Open-File Report, 2010–1280, 1–17, http://pubs.usgs.gov/of/2010/1280/, last access date: 1 December 2016.

Robeson, S. M. 2015. Revisiting the recent California drought as an extreme value. Geophys. Res. Lett. **42**: 6771–6779. doi:10.1002/2015GL064593

Ruesink, J., B. Feist, C. Harvey, J. Hong, A. Trimble, and L. Wisehart. 2006. Changes in productivity associated with four introduced species: Ecosystem transformation of a 'pristine' estuary. Mar. Ecol. Prog. Ser. **311**: 203–215. doi:10.3354/meps311203

Sabine, C. L., and others. 2004. The oceanic sink for anthropogenic CO_2. Science **305**: 367–371. doi:10.1126/science.1097403

Smith, S. V., J. T. Hollibaugh, S. J. Dollar, and S. Vink. 1991. Tomales bay metabolism: C–N–P stoichiometry and ecosystem heterotrophy at the land-sea interface. Estuar. Coast. Shelf Sci. **33**: 223–257. doi:10.1016/0272-7714(91)90055-G

Smith, S. V., and J. T. Hollibaugh. 1997. Annual cycle and interannual variability of ecosystem metabolism in a temperate climate embayment. Ecol. Monogr. **67**: 509–533. doi:10.1890/0012-9615(1997)067[0509:ACAIVO]2.0.CO;2

Sydeman, W. J., M. García-Reyes, D. S. Schoeman, R. R. Rykaczewski, S. A. Thompson, B. A. Black, and S. J. Bograd. 2014. Climate change and wind intensification in coastal upwelling ecosystems. Science **345**: 77–80. doi:10.1126/science.1251635

Waldbusser, G. G., and others. 2016. Slow shell building, a possible trait for resistance to the effects of acute ocean acidification. Limnol. Oceanogr. **61**: 1969–1983. doi:10.1002/lno.10348

Wasson, K. 2010. Informing Olympia oyster restoration: Evaluation of factors that limit populations in a California estuary. Wetlands **30**: 449–459. doi:10.1007/s13157-010-0056-4

Wiltshire, K. H. 2007. Ecophysiological tolerances of the Pacific oyster, *Crassostrea gigas*, with regard to the potential spread of populations in South Australian waters, p. 29. Prepared for the PIRSA Marine Biosecurity. SARDI Aquatic Sciences Publication Number F2007/000499-1. SARDI Research Report Series Number 222. South Australian Research and Development Institute (Aquatic Sciences).

Wootton, J. T., C. A. Pfister, and J. D. Forester. 2008. Dynamic patterns and ecological impacts of declining ocean pH in a high-resolution multi-year dataset. Proc. Natl. Acad. Sci. USA **105**: 18848–18853. doi:10.1073/pnas.0810079105

Yao, H., and X. Hu. 2017. Responses of carbonate system and CO_2 flux to extended drought and intense flooding in a semi-arid subtropical estuary. Limnol. Oceanogr. **62**: S112–S130. doi:10.1002/lno.10646

Acknowledgments

We would like to thank California Sea Grant (R/HCME-02) to EDG and AR for the primary support of this research. We thank J. Largier for sharing equipment and advice; T. Hill, Hog Island Oyster Company, and CENCOOS for providing Burkolator data; D. Dann, H. Stott, and B. Rubinoff for their expert and cheerful field assistance; G. Susner for help making sense of the output of multiple sensors; J. Jennings and the Chemical Analysis Laboratory at Oregon State University for nutrient analyses; and four anonymous reviewers whose comments improved the quality of this manuscript.

Conflict of Interest

None declared.

Submitted 12 July 2018
Revised 01 December 2018; 16 March 2019 and 17 May 2019
Accepted 17 June 2019

Editor: K. David Hambright